Title: *In utero* lipid nanoparticle delivery achieves robust editing in hematopoietic stem cells.

Authors: Atesh K. Worthington[1,2], Beltran Borges[1,2], Tony Lum[1,2], Elisa Schrader Echeverri[3], Fareha Moulana Zada[1,2], Marco A. Cordero[1,2], Hyejin Kim[3], Ryan Zenhausern[3], Ozgenur Celik[3], Cindy Shaw[4], Paula Gutierrez-Martinez[4], Marzhana Omarova[4], Chris Blanchard[4], Sean Burns[4], M. Kyle Cromer[1,2], James E. Dahlman[3], Tippi C. MacKenzie[1,2,5,*]

Authors affiliation

[1] Department of Surgery, University of California, San Francisco, CA, USA

[2] The Eli and Edythe Broad Center of Regeneration Medicine and Stem Cell Research, University of California, San Francisco, CA, USA

[3] Wallace H. Coulter Department of Biomedical Engineering, Georgia Institute of Technology and Emory University School of Medicine, Atlanta, GA, 30332, USA

[4] Intellia Therapeutics, Cambridge, MA

[5] The Center for Maternal-Fetal Precision Medicine, University of California, San Francisco, CA, USA

*Corresponding Author

Abstract:

In vivo genome editing for hematologic malignancies is limited by inefficient delivery of genome editors to hematopoietic stem cells (HSC) in the bone marrow. To overcome this limitation, we capitalized on the inherent liver tropism of lipid nanoparticles (LNPs) and the liver niche of fetal HSCs. We demonstrate that *in utero* delivery of LNPs without active targeting ligands to the fetal liver results in potentially therapeutic levels of HSC editing.

Main Text:

Monogenic hematopoietic disorders could be treated with CRISPR-based genome editing modalities that target hematopoietic stem cells (HSCs) but *ex vivo* strategies have significant limitations such as transplant-related morbidities[1] and cost[2]. Direct *in vivo* genome editing of HSCs could overcome these limitations, however delivery of genome editing reagents to extrahepatic sites (including the bone marrow (BM)) has been challenging. Lipid nanoparticles (LNPs), while effective for *in vivo* editing of hepatocytes[3], have not been efficient for targeting HSCs except when decorated with targeting moieties[4,5]. We hypothesized that HSCs could be edited during a unique developmental window when they reside in the fetal or neonatal liver/circulation. Here we report editing of *bona fide* HSCs after *in utero* or neonatal injection of LNPs without targeting moieties. These results have clinical significance for treatment of severe, early-onset hemoglobinopathies.

We first injected fetal mTmG[6] mice (Cre recombinase results in a switch from TdTomato (Tom) to GFP expression) at embryonic age (E) 13.5-14.5 with 1.5-3 mg/kg LNP[67] (previously reported to be HSC-tropic[7]) packaged with mRNA encoding Cre recombinase (**Fig. 1A**). We analyzed HSC transfection using flow cytometry between E18.5 and P3 and observed robust transfection at the 3 mg/kg dose (**Fig. 1B,C**), albeit at lower frequencies than in the liver (**Fig. 1D**). To determine whether transfected HSCs are functional, we sorted GFP+ liver HSCs after 4-5 days

(or Tom+ HSCs from uninjected age-matched controls) and transplanted into sublethally irradiated wild-type recipients (**Fig. 1E**). We observed similar levels of multilineage engraftment between GFP+ and Tom+ HSCs in the blood (**Fig. 1F**) and in the BM (**Fig. 1G**), confirming that LNP-transfected HSCs are definitive HSCs.

We next investigated whether LNPs could deliver Cas9 mRNA and gRNA to mediate efficient editing in fetal or neonatal HSC, using a Cas9 reporter mouse (Traffic Light Reporter, TLR[8]). In TLR mice, repair of Cas9-induced double-stranded breaks with insertions or deletions (InDels) can restore the reading frame of an RFP transgene (**Fig. 2A**). Analysis of adult BM HSCs after *in utero* injection of 3 mg/kg LNP-Cas9 demonstrated robust editing by flow cytometry, up to 15-30% in some animals (**Fig. 2B,C**). Interestingly, HSC editing was also detected after injection of LNP-Cas9 in P0 mice, albeit at lower levels than after *in utero* injection, suggesting that the time window for accessing HSCs extends beyond the prenatal period (**Fig. 2C**). Rates of HSC editing were similar to those in the liver after in utero, but not neonatal injection (**Fig 2D)**. Notably, RFP expression under-represents editing levels, due to the requirement of in-frame editing to restore RFP expression, as evidenced by higher levels of editing (~3-fold) detected by Sanger sequencing compared to flow cytometry (**Fig. 2E**). To test HSC function, we sorted edited (RFP+) hematopoietic stem and progenitor cells (HSPC; Lin-cKit+Sca+) BM of LNP-injected animals and transplanted into irradiated wild-type recipients (**Fig. 2G**). We detected robust engraftment of RFP+ cells with multilineage reconstitution in the blood (**Fig. 2H**) and HSC engraftment in BM (**Fig. 2I**), confirming that *in vivo* editing does not impact HSC function.

These data represent proof-of-concept support for the promise of direct *in vivo* editing of HSCs in the fetal liver or neonatal circulation. Levels of editing achieved with LNP-Cas9 in some experimental animals were at levels that could be effective to treat hemoglobinopathies[9]. While *in utero* injection appears more effective that postnatal, *bona fide* HSCs can also be edited with the latter method, suggesting the time window for achieving a “one-and-done” treatment for severe, early-onset hematologic conditions may extend into early neonatal life, when HSCs are in the circulation[10]. Moreover, robust editing of HSCs during this time period can be achieved using LNPs that are not specifically targeted with antibodies. Given the expansion of interest in prenatal diagnosis and therapies, particularly for diseases in which editing of HSCs could be curative[11], our results are an important first step for considering early (fetal or neonatal) somatic cell genome editing as a modality for further research.

References:

1. Charlesworth, C. T., Hsu, I., Wilkinson, A. C. & Nakauchi, H. Immunological barriers to haematopoietic stem cell gene therapy. *Nat Rev Immunol* **22**, 719–733 (2022).

2. Sheridan, C. The world’s first CRISPR therapy is approved: who will receive it? *Nature Biotechnology* **42**, 3–4 (2023).

3. Gillmore, J. D. *et al.* CRISPR-Cas9 In Vivo Gene Editing for Transthyretin Amyloidosis. *N Engl J Med* **385**, 493–502 (2021).
4. Breda, L. *et al.* In vivo hematopoietic stem cell modification by mRNA delivery. *Science* **381**, 436–443 (2023).
5. Palanki, R. *et al.* In utero delivery of targeted ionizable lipid nanoparticles facilitates in vivo gene editing of hematopoietic stem cells. *Proc Natl Acad Sci U S A* **121**, e2400783121 (2024).
6. Muzumdar, M. D., Tasic, B., Miyamichi, K., Li, L. & Luo, L. A global double-fluorescent Cre reporter mouse. *Genesis (New York, N.Y. : 2000)* **45**, 593–605 (2007).
7. Kim, H. *et al.* Lipid nanoparticle-mediated mRNA delivery to CD34+ cells in rhesus monkeys. *Nat Biotechnol* (2024) doi:10.1038/s41587-024-02470-2.
8. Chu, V. T. *et al.* Increasing the efficiency of homology-directed repair for CRISPR-Cas9-induced precise gene editing in mammalian cells. *Nat Biotechnol* **33**, 543–548 (2015).
9. Hoban, M. D. *et al.* CRISPR/Cas9-Mediated Correction of the Sickle Mutation in Human CD34+ cells. *Mol Ther* **24**, 1561–1569 (2016).
10. Christensen, J. L., Wright, D. E., Wagers, A. J. & Weissman, I. L. Circulation and chemotaxis of fetal hematopoietic stem cells. *PLoS Biol* **2**, E75 (2004).
11. Chu, S. N. *et al.* Dual α-globin-truncated erythropoietin receptor knockin restores hemoglobin production in α-thalassemia-derived erythroid cells. *Cell Rep* **44**, 115141 (2025).
12. Nijagal, A., Le, T., Wegorzewska, M. & Mackenzie, T. C. A mouse model of in utero transplantation. *J Vis Exp* 2303 (2011) doi:10.3791/2303.
13. Gombash Lampe, S. E., Kaspar, B. K. & Foust, K. D. Intravenous injections in neonatal mice. *J Vis Exp* e52037 (2014) doi:10.3791/52037.
14. Kulandavelu, S. *et al.* Embryonic and neonatal phenotyping of genetically engineered mice. *ILAR J* **47**, 103–117 (2006).

15. Worthington, A. K. *et al.* IL7Rα, but not Flk2, is required for hematopoietic stem cell reconstitution of tissue-resident lymphoid cells. *Development (Cambridge, England)* **149**, (2022).

16. Leung, G. A. *et al.* The lymphoid-associated interleukin 7 receptor (IL7R) regulates tissue-resident macrophage development. *Development (Cambridge)* **146**, (2019).

17. Chen, D. *et al.* Rapid discovery of potent siRNA-containing lipid nanoparticles enabled by controlled microfluidic formulation. *J Am Chem Soc* **134**, 6948–6951 (2012).

18. Belliveau, N. M. *et al.* Microfluidic Synthesis of Highly Potent Limit-size Lipid Nanoparticles for In Vivo Delivery of siRNA. *Mol Ther Nucleic Acids* **1**, e37 (2012).

19. Beaudin, A. E. *et al.* A Transient Developmental Hematopoietic Stem Cell Gives Rise to Innate-like B and T Cells. *Cell stem cell* **19**, 768–783 (2016).

Figure Legends:

Figure 1. *In utero* LNP delivery results in transfection of *bona fide* HSCs. A) Experiment schematic. **B)** Gating strategy to identify LNP-transfected HSCs (Lin- cKit+ Sca+ SLAM+ GFP+). **C)** % GFP+ liver HSCs. 1.5 mg/kg (n=4), 3 mg/kg (n=21). P= not significant (NS) (Student's t-test). **D)** Frequency of GFP+ liver cells vs. HSCs in livers of LNP-injected mice (3 mg/kg, n=21). ****P<0.0001 (Paired student's t-test). **E)** Experiment schematic of HSC transplants after isolating GFP+ HSCs as presented in 1C. **F)** % GFP+ (green circle, n=7) and Tom+ (red squares, n=8) granulocyte and macrophages (GM), B cells and T cells in blood of transplanted mice weeks post-transplant. P=NS between mean GFP+ vs Tom+ at each time point by Student's t-test. **G)** % donor-derived HSCs (solid bars) and multipotent progenitors (MPPs, patterned bars, Lin-cKit+Sca+SLAM-Flk2+) in BM of GFP+ (green bars) and Tom+ (red bars) HSC transplanted mice 16+ weeks post-transplant. P=NS between mean GFP+ vs Tom+ HSC or MPP (Student's t-test). Data are mean+/-SEM; each dot represents an individual animal, least 2 independent experiments.

Figure 2. *In utero* or neonatal injection of LNPs carrying Cas9/gRNA results in editing of HSCs. A) Experiment schematic. E13.5 TLR mice were injected intrahepatically with LNP-Cas9/gRNA. BM and livers were harvested in adult mice. **B)** Gating strategy to identify Cas9-edited HSCs (Lin- cKit+ Sca+ SLAMmid/hi RFP+). **C)** % RFP+ HSCs in BM of mice injected *in utero* (n=8) or postnatally (n=8) with 3 mg/kg of LNP. *P<0.05 (Mann-Whitney test). **D)** % RFP+ liver cells vs HSCs in the BM of in utero and postnatally injected mice. ***P<0.005 (Paired student's t-test). **E)** Comparison of % editing in liver cells quantified by RFP expression (by flow) or InDel frequency (by Sanger sequencing). ****P<0.0001 (Paired student's t-test). **F)** Fold-change of % InDel vs. RFP in liver cells in adult mice after *in utero* and postnatal injection. P=NS (Student's t-test). **G)** Experiment schematic of HSC transplants. RFP+ HSCs were isolated from postnatally injected animals presented in 1E. **H)** Percentage of RFP+ (n=10) GM, B cells and T cells in blood of transplanted mice weeks post-transplant. **I)** Percentage of donor-derived HSCs (solid bars) and MPPs (patterned bars) in BM of RFP+ HSPC transplanted mice 16+ weeks post-transplant. Data are mean+/-SEM; each dot represents an individual animal.

Methods:

Mouse Husbandry and Injections:

Mouse husbandry and procedures were performed according to the UCSF Institutional Animal Care and Use Committee-approved protocol AN202125-00B. mTmG (strain #007676) and TLR (strain #034033) mice were purchased from Jackson (Jax) Laboratories. Prenatal intrahepatic injections were performed as previously described[12]. Neonatal temporal vein injections were performed as previously described[13]. In utero and postnatal injection were dosed with same mg/kg of LNP based on previously published embryonic weights of C57Bl6 mice[14] and weights at birth.

Tissue harvesting

Mice were euthanized by CO_2 inhalation and transcardially perfused with PBS. Livers, leg and hip bones were processed as previously described[15,16]. Briefly, bone marrow was isolated by crushing and filtering. Livers were minced into 2mm x 2mm pieces and digested in 1mg/mL collagenase IV for 45 minutes, then passaged through a 19 g needle ten times, and then filtered through a 70 µm filter.

LNP[67] Formulation:

Cre recombinase mRNA was diluted in 25 mM sodium acetate buffer, while the remaining lipid components were diluted in 100% ethanol. The phases were then microfluidically mixed[17,18] using NanoAssemblr Ignite (Precision Nanosystems) at a relative flow rate of 3:1 (RNA and lipid phases, respectively) and 12ml/min total flow rate. LNPs were diluted 1:42 in sterile 10mM Tris buffer and dialyzed by centrifugation in 100 kDa ultra centrifuge tubes (Amicon) at 4°C. Sucrose (NF, EP, JP, ChP, high purity, low endotoxin, Fisher Scientific) was dissolved in a sterile 10 mM Tris buffer at 60% (w/v). LNPs in 10 mM Tris buffer were mixed with 60% (w/v) sucrose solution at 5:1 (v/v LNP:sucrose) for the final concentration of sucrose at 10% (w/v). LNPs were then flash-frozen in liquid nitrogen. Frozen LNPs were stored at ≤ −80°C. To thaw, LNPs were incubated at room temperature for 20 min. The LNPs were sterile-filtered with 0.22-µm filter before administration.

LNP-Cas9/gRNA Formulation:

LNPs containing gRNA and Cas9 mRNA were manufactured by a controlled mixing process to encapsulate the gRNA and Cas9 mRNA in LNPs. In addition to the RNA components, the LNPs are composed of four lipids including an ionizable lipid, a phospholipid, a pegylated lipid and cholesterol. After mixing, the LNPs were purified and buffer exchanged into an aqueous storage buffer. LNPs were characterized using RiboGreen (Thermo Fisher) and dynamic light scattering to determine cargo concentration, encapsulation efficiency, and size. LNPs had encapsulation efficiencies above 95% and z-average diameters between 70-95 nm.

Flow cytometry and FACS:

Cell labeling was performed on ice in 1× PBS with 5 mM EDTA and 2% serum. Antibodies used are listed in Table S1 below. Analysis and cell sorting was performed on BD LSRII and BD FACS Aria II and analyzed using FlowJo. Cells were defined as follows as previously reported[15,19]: Granulocytes/Macrophages (Gr-1+ Mac-1+ B220- CD3- Ter119- CD61-); B cells (B220+ CD3- Gr-1- Mac-1- Ter119- CD61-); T cells (CD3+ B220- Gr-1- Mac-1- Ter119- CD61-); fetal/neonatal HSCs (Lin-cKit+Sca+SLAM+), adult HSC (Lin-cKit+Sca+SLAMmid/hi Flk2-), adult MPP (Lin-cKit+Sca+SLAM- Flk2+), HSPC (Lin-cKit+Sca+).

Antibody	Source	Identifier	Dilution
B220-APC Cy7	Biolegend	103224	1:400
CD3-A700	Biolegend	100216	1:200
Mac-1-PE Cy7	Biolegend	101216	1:400
Gr-1-Pacific Blue	Biolegend	108430	1:400
Ter119-PE Cy5	Biolegend	116210	1:400
CD61-A647	Biolegend	104314	1:400
B220-A700	Biolegend	103231	1:400
Mac-1-A700	Biolegend	101222	1:400
Gr-1-A700	Biolegend	108421	1:400
Ter119-A700	Biolegend	116220	1:400
cKit-APC Cy7	Biolegend	105826	1:400
Sca-1-Pacific Blue	Biolegend	122520	1:400
SLAM-PE Cy7	Biolegend	115914	1:400
Flk2-APC	Biolegend	135310	1:100

Transplantation experiments:

Transplantation assays were performed as previously described[15]. Briefly, single purity sorted HSCs or HSPCs were isolated from liver or bone marrow of LNP-injected mice. Lineage markers were CD3, B220, Mac1, Gr1 and Ter119. Mac1 antibodies were excluded from the lineage cocktail when sorting fetal HSCs. Recipient mice aged 8-12 weeks were sublethally irradiated (500 rad for HSC transplants and 700 rad for HSPC transplants, single dose) with a Faxitron CP-160 and sorted cells were transplanted retro-orbitally. Donor chimerism in peripheral blood of recipients was analyzed by flow cytometry.

Polymerase Chain Reaction (PCR) and Sanger sequencing:

Genomic DNA was extracted from snap-frozen tissues using DNeasy Blood and Tissue kit (QIAGEN, catalog #69504) per manufacturer's instructions, quantified using a nanodrop, and amplified using Phusion Green PCR MasterMix (ThermoFisher, catalog #F-566L) and the primers outline in Table S2. Thermocycler (Bio-Rad) settings were as follows: 98 °C (30 s), 98 °C (10 s), 72º C (30 s), 72 °C (30 s), return to step 2 for 34 cycles and then 72 °C (10 s). PCR products were purified using SPRIselect Beads (Beckman-Coulter, catalog #B23317) per manufacturer's instructions, re-quantified using a nanodrop, and sent for sequencing

(QuintaraBio). Sequencing (.ab1) files were analyzed using Synthego ICE software to determine indel percentage.

Table S2. Primers used for PCR and Sanger Sequencing

	Primer Name	Primer Sequence
PCR	TLR_F2	5'- ATG GTG AGC AAG GGC GAG GA -3
	TLR_R2	5'-CTT GTA CAG CTC GTC CAT GC - 3'
Sequencing	TLR_R2	5'-CTT GTA CAG CTC GTC CAT GC - 3'
	gRNA	TTGCAGCTCGAACTTCACCT

Acknowledgements

This work was supported by NIH R01 HL161291 to T.C.M. We acknowledge the UCSF Parnassus Flow Cytometry Core (RRID:*SCR_018206*) supported in part by Grant NIH P30 DK063720 and by the NIH S10 Instrumentation Grant S10 1S10OD021822-01. We thank all the members of the MacKenzie lab, Dahlman lab and Cromer lab for helpful discussion.

Author contributions

A.K.W. and T.C.M conceptualized the study. A.K.W, B.B., T.L., F.M.Z., M.A.C. performed all experiments. E.S.E., R.Z., O.C., H.K., C.S., P.G.M., M.O., C.B., S.B. and J.E.D. formulated the LNPs. A.K.W., B.B. and M.K.C. analyzed the data. A.K.W. prepared the figures. A.K.W. and T.C.M wrote the manuscript with input from all authors.

Competing interests

T.C.M. is on the scientific advisory board of Acrigen and receives grant funding from Novartis, BioMarin, and Biogen. J.E.D. is an advisor to GV, Readout, Edge Animal Health and Nava Therapeutics. C.S., P.G.M, M.O., C.B., S.B are/were employees of Intellia Therapeutics. None of these companies provided any financial support for this work. The other authors declare no competing interests.

Figure 1. *In utero* LNP delivery results in transfection of *bona fide* HSC.

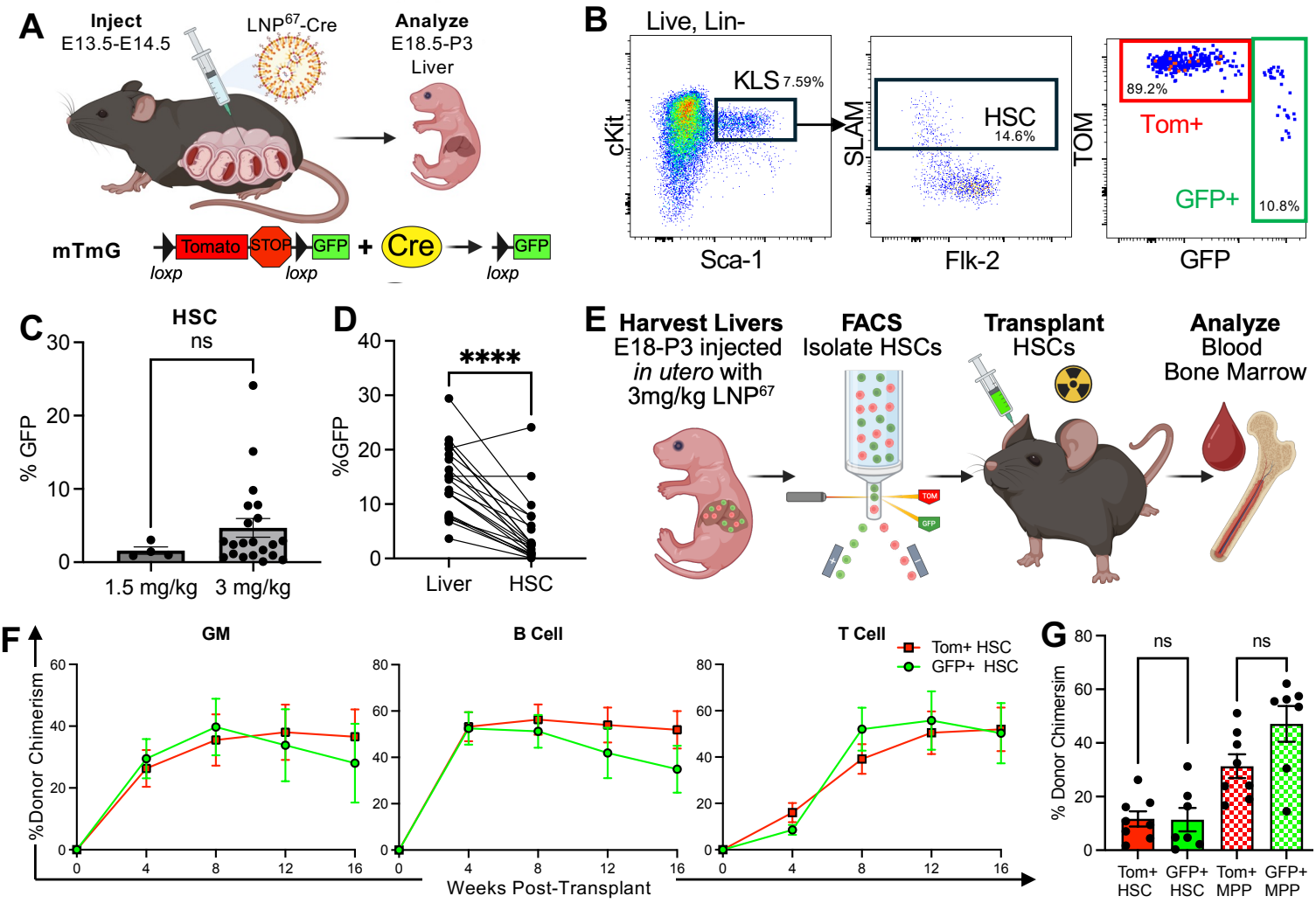

Figure 2. *In utero* or neonatal injection of LNPs carrying Cas9/gRNA results in editing of HSCs.